Rev. Adv. Mater. Sci. 48 (2017) 147-155

STABILIZATION OF CUBIC ZIRCONIA BASED SOLID SOLUTIONS OBTAINED BY CRYOCHEMICAL TECHNIQUES: THERMODYNAMIC AND KINETIC FACTORS

O.Yu. Kurapova[1,2], S.N. Golubev[2], V.M. Ushakov[2] and V.G. Konakov[1,2]

[1]St. Petersburg State University, St. Petersburg, 199034, Russia
[2]Glass and Ceramics Ltd., St. Petersburg, 199004, Russia

Received: November 12, 2016

Abstract. The work reports the detailed investigation of factors affecting crystallization and phase stability of nanosized precursors based on zirconia solid solutions obtained by reversed co-precipitation technique from diluted salts solution and further dehydration (freeze-drying, freeze-drying with glycerol, freezing in liquid nitrogen, drying under overpressure). Basing on simultaneous thermal analysis (STA) data, the criterion for crystallization completeness of the "amorphous phase → crystalline solid solution" transition was suggested. Consideration of STA and X-Ray diffraction technique (XRD) results provides an opportunity to state that freeze-drying favors step character of precursor crystallization, while the use of freezing in liquid nitrogen leads to single step crystallization. Combining XRD results with the data of particle size distribution analysis, it was shown that phase stabilization of cubic zirconia based solid solution at temperatures up to 1000 °C is due to the fine powder dispersity in that temperature region.

1. INTRODUCTION

The investigation of phase transformation sequences "amorphous phase → metastable crystalline solid solution → equilibrium crystalline phase" in nanosized systems is of great applied and fundamental importance for the development of the advanced materials possessing regulated physical and chemical characteristics. Nanosized precursors based on cubic zirconia solid solutions gain special attention as they are actively used for the manufacturing of the anion-conducting nanoceramics [1], oxygen sensors [2,3] and membranes for solid oxide fuel cells (SOFC) [4]. In some amounts, these nanosized precursors are also used as dopants for novel metal matrix (Ni, Al) composites [5] as well as for a number of special materials: polymer thermal insulation for liquefied gas transportation, spheroplasts, etc.

I.A. Ovid'ko contributed much into the development of the fundamentals of mechanical properties of nanoceramics and ceramic based composites [6,7]. The theoretical predictions made were successfully confirmed by the fruitful collaboration of groups of Prof. Ovid'ko and Prof. Konakov [8-11]. At the same time the applicability of such ceramics and ceramic powders is limited by certain criteria. Stabilization of zirconia in a form of cubic solid solution is one of the main criteria for such nanosized powders applicability for the advanced materials fabrication since the use of low symmetric ZrO_2 modifications (monoclinic and tetragonal) here does not allow reaching the required materials characteristics. ZrO_2 doping by alkaline earth and rare-earth metal oxides results in cubic solid solutions formation and the anionic vacations generation in their crystal lattice. From the positions of thermodynamics, the temperature and phase stability region of

Corresponding author: O.Yu. Kurapova, e-mail: olga.yu.kurapova@gmail.com

cubic zirconia based solid solutions depend on the nature and amount of the doping oxide, see, for example [12-14]. However, it is known [15,16] that the use of bottom-up approach like sol-gel synthesis and cryochemical dehydration of gels obtained allows also metastable zirconia modifications production due to the phase transition "amorphous precursor → metastable crystalline solid solution". The temperature and concentration limits of phase stability region for the metastable solid solution here is affected by a number of kinetic factors, such as dispersity of powders obtained, annealing duration and temperature, and crystallite size in powders. Since the surface energy effect is very significant in nanosystems, one should consider its effect on the shift of phase transitions tempera-tures, thermodynamic properties of solid solution formed, and the interaction between the oxide components in case of nanosized zirconia powders [17]. We should mention that stable solid solutions formation and their properties are widely discussed in literature, see e.g. [18-20]. At the same time, the factors affecting the emergence and phase stability of nanocrystalline zirconia solid solutions are poorly understood. Therefore, the goal of the present work is the consideration of thermodynamic and kinetic factors on the temperature of "amorphous phase → metastable crystalline solid solution" transition and phase stability of cubic zirconia solid solution with CaO content of 5-15 mol.% formed in the temperature range 400-1300 °C.

2. EXPERIMENTAL

2.1. Synthesis

Nanosized calcia stabilized zirconia powders were obtained by reversed co-precipitation from diluted aqueous salt solutions. The compositions with CaO content 5, 9, 12, and 15 mol.% (compositions I, II, III, and IV, respectively) were chosen according to CaO-ZrO_2 phase diagram [17]. Commercially available hydrates $ZrO(NO_3)_2 \cdot 2H_2O$ and $Ca(NO_3)_2 \cdot 2H_2O$ were used to prepare 0.1M aqueous solution. 1M ammonium aqueous solution was used as a precipitant. Mixed salt solution was added to NH_4OH by drops with a rate of ~ 2 ml/min. The precipitation has been performed at ~1-2 °C in an ice bath at constant stirring; pH of the solution was kept at ~9-10 during the synthesis by means of ammonium solution addition. To remove reaction byproducts, the obtained gels were filtered and rinsed until the neutral pH was reached. The obtained gels underwent different unidirectional freezing via freeze-drying, freeze-drying with 10 wt.% of glycerol, freezing in liquid nitrogen, pan drying under overpressure (treatments types 1, 2, 3, and 4, respectively).

2.1.1. Freeze-drying

To perform freeze-drying, thin layers of gels I - IV were deposited to Petri dish surface and then were rapidly frozen at -50 °C with the cooling rate of 1-2 °C/min. Frozen samples were then freeze-dried using Labconco 1L chamber (0.018 Torr, 20 °C, 24 hours).

2.1.2. Freeze-drying with glycerol

In this approach, glycerol was used as a cryoprotectant in order to protect gels from possible damage caused by freezing, the typical type of such damage is cracking. The amount of glycerol addition was 10 wt.%, this optimal type and amount of cryoprotectant were chosen in accordance with the recent research of the authors [21]. The samples of I-IV gel compositions were prepared and freeze-dried with glycerol similarly to specimens described above (see Section 2.1.1).

2.1.3. Freezing in the liquid nitrogen

To perform freezing in liquid nitrogen, the gel, by small portions, was placed into Dewar flask filled by liquid nitrogen under mechanical stirring. The stirring is necessary to reach homogeneous gel freezing since the layer of solidified gel formed on the liquid nitrogen surface blocks the contact between gel and liquid nitrogen. After liquid N_2 evaporation, the frozen granules were left at the ambient conditions for dispersed medium evaporation.

2.1.4. Pan drying under exceeded pressure

Thus obtained gels were pan dried overpressure (5 kg/m^2) between two chemically inert smooth surfaces (glass plates) at 130 °C for ~15 min.

All precursors obtained via different dehydration techniques were annealed at 400, 600, 800, 1000, and 1300 ° for 3 hours. Table 1 lists the manufactured specimens, here and after the composition is in mol.%.

2.2. Analysis

In order to understand the effect of thermal treatment, all the samples were studied by Simultaneous

Thermal Analysis (STA, Netzsch STA 449 F1 Jupiter) including differential scanning calorimetry (DSC) and thermal gravimetry (TG). The measurement were carried out in nitrogen ambience with the scanning rate of 10 °C/min in the temperature range was 20-1200 °C. Phase composition of the thermally treated samples was determined using X-Ray diffraction analysis (XRD, Shimadzu XRD-6000). XRD of the samples has been performed in air at room temperature using Cu Kα radiation, λ = 1.54 Å. The average crystallite size was estimated from the most intensive reflex profile using Scherrer's formula. The dispersity of the precursor powders was studied using particle-size distribution analysis (PSD, Horiba Partica LA-950 laser analyzer). The mean size of the powder particles was calculated from powder size distributions obtained. The residual amount of glycerol in the powders after freeze-drying was determined using Fourier transform infrared spectroscopy (FTIR, Nicolet iS 50 FT-IR Spectrometer).

3. RESULTS AND DISCUSSION

The DSC curves obtained for precursor I-IV obtained by different gel dehydration approaches are shown in Fig. 1. One can see that three main regions can be distinguished in each DSC curve: endothermic effect in the region from 50 to 250 °C corresponding to the dehydration and two exothermic effects at ~360 and at 490-550 °C, they are attributed to the amorphous precursors crystallization. Extended endothermic effects indicate that the dehydration process is gradual. The completeness of dispersed medium (water) removal from the gels is independent of precursor composition, but depends on dehydration technique chosen. Table 1 lists the data on temperatures of dehydration peaks in DSC curves for precursors I-IV and the mass losses in the temperature range below 400 °C.

For all precursors obtained by cryochemical dehydration (freeze-drying, freeze-drying with glycerol, freezing in the liquid nitrogen), the formation of anhydrous $x\mathrm{ZrO_2}(100\text{-}x)\mathrm{CaO}$ is related to the continuous change of condensed phase composition. Note that two endothermic peaks are clearly observed in DSC curves of precursors I.4 and IV.4 treated by pan drying under overpressure. This fact indicates that the mass losses of dispersed (adsorbed) and structurally bounded water (water in a form of hydroxides) occur sequentially. The amount of residual water in specimens I.4-IV.4 varies significantly depending on the sample composition, it lies in the range from 17.8 to 25.9 wt.%, see Table 1. The maximum of the dehydration temperature in the DSC curves of the precursors obtained by freezing in the liquid nitrogen can be estimated as 116 °C. That allows assuming that a significant amount of dispersed water presents in the samples. Indeed, water losses in precursors I.3-IV.3 lies in the range from 35 to 49 wt.%, which corresponds to formula $x\mathrm{Ca(OH)_2}(100\text{-}x)\mathrm{Zr(OH)_4}{*}n\mathrm{H_2O}$, where x= 0.05, 0.09, 0.12, 0.15 and n=0.75-1.64. It should be noted that cryoprotectant addition leads to the shift of the maximum of the endothermic effect to the high temperature region. Glycerol is a simplest trihydric alcohol. Its reactivity is determined by two secondary and one primary hydroxyl groups [22]. Since glycerol possesses weak base properties, it

Table 1. Temperatures of the endothermic peaks on DSC curves of precursors I-IV after different dehydration and mass losses in the temperature range below 400 °C. For samples I-4 and IV-4 there are 2 peaks of dehydration.

	I		II		III		IV	
	$T_{dehydr,}$ °C	Δm, wt. %	$T_{dehydr,}$ °C	Δm, wt. %	$T_{dehydr,}$ °C	Δm, wt. %	$T_{dehydr,}$ °C	Δm, wt. %
1. Freeze-drying	161.7	21.4	131.5	24.8	140.8	25.1	133.9	25.05
2. Freeze-drying with 10 wt.% of glycerol	165.1	23.3	136.1	24.8	158.9	24.7	167.2	20.18
3. Freezing in liquid nitrogen	117.7	47.25	134.6	34.7	116.1	41.09	116.0	49.24
4. Drying under overpressure	122.5 178.1	25.9	130.4	17.8	126.9	22.1	133.6 168.1	24.08

Table 2. Crystallization temperatures and entalpy of crystallization of powders according to DSC data.

	freeze-drying		freeze-drying with 10 wt.% of glycerol		freezing in the liquid nitrogen		pan drying under exceeding pressure	
	$-\Delta H$, J/g	T_{cryst}, °C	$-\Delta H$, J/g	T_{cryst}, °C	$-\Delta H$, J/g	T_{cryst}, °C	$-\Delta H$, J/g	T_{cryst}, °C
I	139.6±14	562	140.4±14	583	145.5±15	572.5	126.8±13	545
II	162.22±14	494	161.0±16	502	165.2±17	493	167.2±17	500
III	296±14	513	141.3±14	535	100.9±10	553.5	103.7±10	524
IV	125.86±14	610	129.4±13	608	132.5±13	610	124.2±12	606

is possible to assume the formation of complex calcium glycerate. Water in such glycerate is more tightly bound than in calcium and zirconium hydroxides. That is, likely, the reason for the temperature shift observed. According to FTIR data, the amount of residual glycerol in freeze-dried powders is <0.84 g/mol. Therefore, the mass losses at temperatures ≤400 °C in case of precursors processed by freeze-drying with glycerol can be completely attributed to water losses. The quantitative comparison of water losses from dehydrated precursors shows that the total mass losses values within the chosen dehydration techniques are similar and do not depend on the precursor composition. Analysis of the presented in Table 1 shows that cryochemical dehydration affects the initial precursor structure less than pan drying under overpressure.

The exothermic effect at 490-560 °C in DSC curves (see Fig. 1) corresponds to phase transformation "amorphous precursor → metastable crystalline solid solution". The summarized data on the temperatures of amorphous phase crystallization are listed in Table 2. The temperature of exothermic peaks corresponding to crystallization differs within

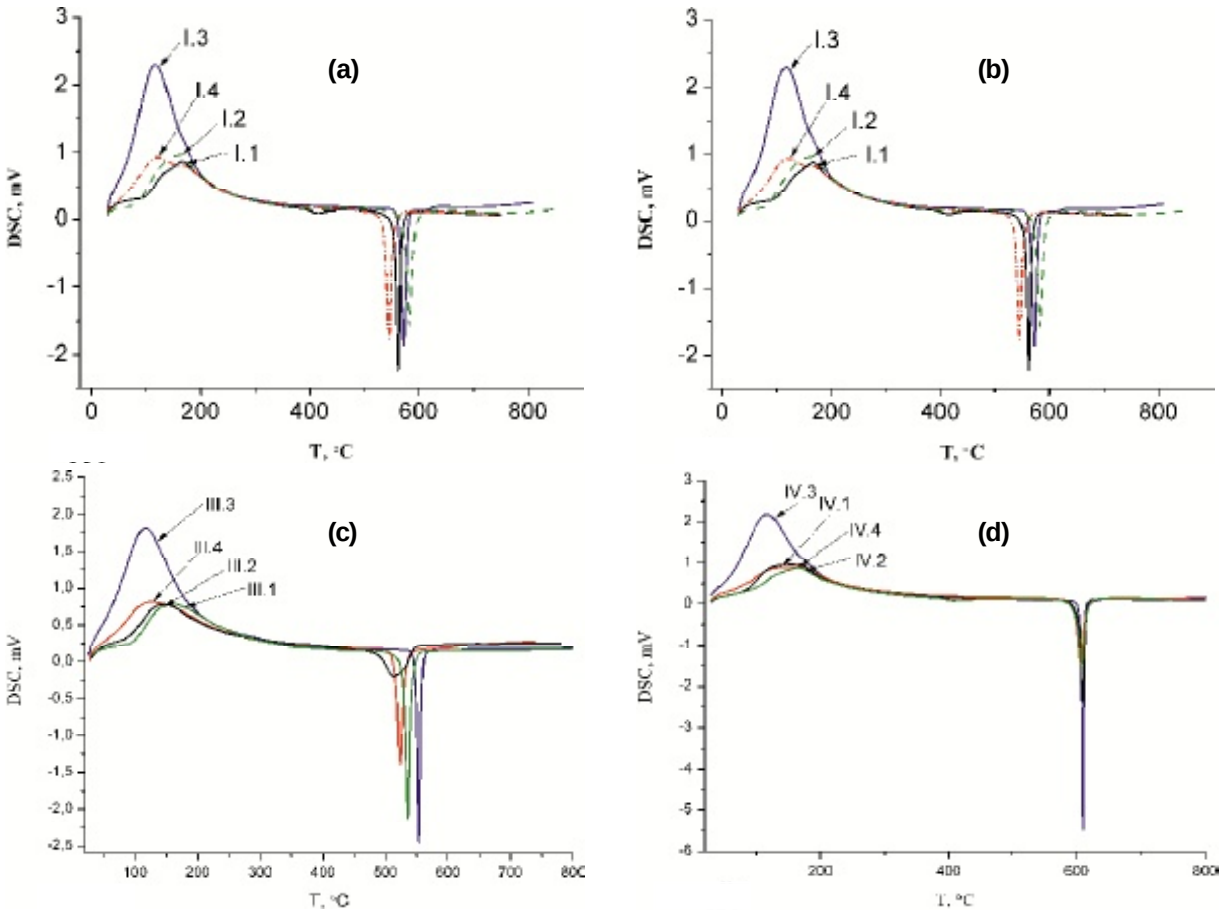

Fig. 1. DSC curves obtained for precursors (a) I, (b) II, (c) III and (d) IV after different dehydration processes.

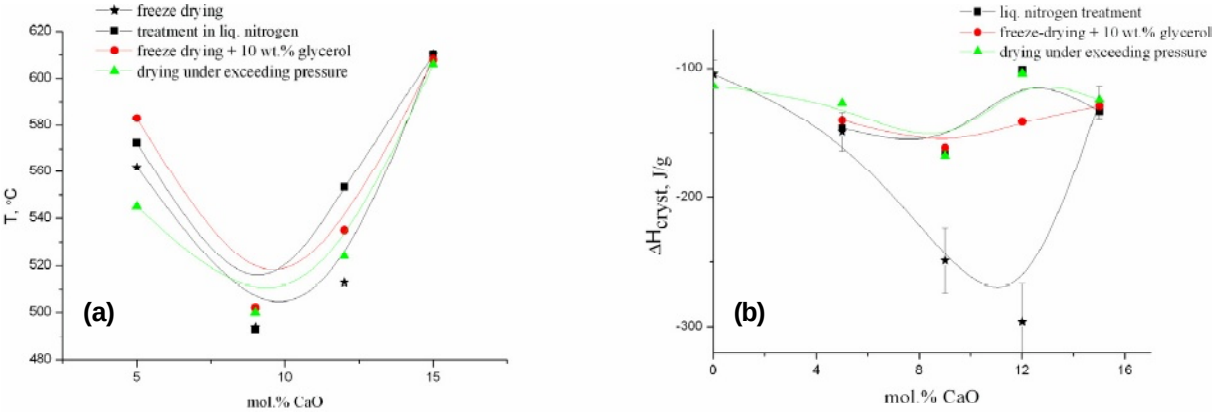

Fig. 2. The dependence of (a) crystallization temperature and (b) crystallization enthalpy on precursors composition.

20 °C for all specimens. Such a narrow interval of crystallization temperatures suggests the similar structure of powders as well as similar mean agglomerate size. The dependence of the exothermic effect temperature on precursor composition was plotted (see Fig. 2a and Table 1). As seen from the figure, the temperature of metastable cubic zirconia solid solution formation is determined by dopant amount and it is minimal in case of 9 mol.% CaO addition. Since the enthalpy of any process is the measure of process affinity, given ΔH value allows estimating the structural difference of the powders obtained by four dehydration techniques, so, these crystallization enthalpy values were calculated from DSC data. It should be noted that in case of freeze-dried precursors I.1 and II.1 one more exothermic effect is observed at 410 and 360 °C, respectively. As it was shown earlier in [23], the effect corresponds to low-temperature crystallization of cubic solid solution. Since the enthalpy is an additive value, the total enthalpy of crystallization process can be written as

$$\Sigma\Delta H = \Delta H_{prior} + \Delta H_{cryst}, \quad (1)$$

where ΔH_{prior} is the enthalpy of low-temperature crystallization at 360-410 °C and ΔH_{cryst} - the crystallization enthalpy at 490-550 °C. Calculated values of crystallization enthalpy for precursors I.1 and II.1 were -8.7±1 and -34±3 J/g, respectively. Using Eq. 1, the total value of crystallization enthalpy of the freeze-dried precursors was calculated, its dependence on precursor composition is demonstrated in Fig. 2b. The value of crystallization enthalpy for undoped ZrO_2 obtained in our recent work [24] was used here.

As seen from Fig. 2b, all the dehydration technique except freeze-frying without cryoprotectant addition demonstrated crystallization enthalpies nearly independent of precursor composition with the mean value of -164±16 J/g. The curve has the extreme nature in case of freeze-dried powders. The value of $\Sigma\Delta H$ decreases and reaches its minimum in case of Specimen III (12CaO-88ZrO_2). That indicates that the crystallization of composition III is likely the most complete comparing to the others. Analyzing the obtained data on the change of crystallization enthalpy, one can assume that the observed difference is due to different initial structure of powders after synthesis. The less system is thermally affected during dehydration, the more significant rearrangement is needed during the crystallization. Indeed, the recent work of the authors [25] demonstrated that freeze-drying with no additives results in the ordered three-dimensional network formation. This network comprised of nonporous particles and its structure is similar to the initial structure of the gel. At the same time, powders comprised of dendritic agglomerates were obtained after freezing in liquid nitrogen and pan drying under overpressure. Pan drying technique favors primary crystallites formation during dewatering at 110 °C, and, as it was shown in [26], the careful optimization of dehydration conditions allows obtaining the crystallites with the mean size equal to particle size of dispersed phase.

In order to investigate the crystallization process and phase formation in precursors with temperature, the powders were annealed at 400-1300 °C for 3 hours. XRD patterns of freeze-dried precursors I-IV annealed at 400 °C are presented in Fig. 3a. As seen from the figure, the crystallization at the temperature prior the main exothermic effect on DSC curve takes place for all the compositions except Specimen IV. At the same time, powders

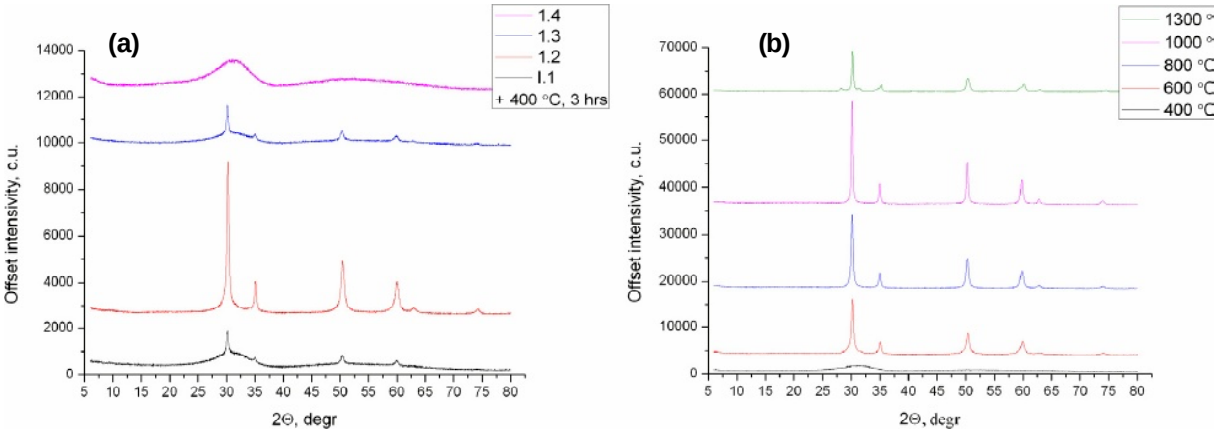

Fig. 3. XRD patterns of (a) freeze-dried precursors I-IV annealed at 400 °C, 3 hours and (b) precursor IV after annealing at 400-1300 °C, 3 hours.

after dehydration by pan drying at the overpressure and freezing in liquid nitrogen are still X-ray amorphous. XRD data obtained are in accordance with composition dependencies of crystallization temperature and enthalpy change of the process. That allows suggesting the value of crystallization enthalpy of the phase transition "amorphous precursor → crystalline solid solution" as the criterion for crystallization completeness of metastable cubic solid solutions in CaO-ZrO_2 system.

It is interesting to note that similar phase formation behavior was observed in case of annealed precursors after freeze-drying with 10 wt.% glycerol addition. However, the change in crystallization enthalpy for precursors I.2-IV.2 is independent of CaO amount. Let us consider the change of the Gibbs energy of crystallization as

$$\Delta G_{crypt} = \Delta H_{crypt} - T\Delta S_{crypt}. \quad (2)$$

Basing on DSC and XRD data, calculated ΔH_{cryst} values, and Eq. (2) consideration, one can assume that the driving force of low temperature crystallization in case of freeze-dried precursors is the enthalpy change, while in case of freeze-dried with glycerol powders this driving force is the entropy change. The step character of crystallization is confirmed by the data on the enthalpy obtained. The temperature increase favors cubic zirconia based solid solution formation for all precursors. The phase formation is in accordance with empiric Ostwald step rule on preferable crystallization of high symmetric phases. As an example, XRD patterns of precursor IV.1 annealed at different temperatures are presented in Fig. 3b. The incorporation of at least 9-15 mol. % CaO in ZrO_2 combined with the use of cryochemical techniques favors stability of cubic zirconia based solid solution in the range 400-1000 °C. At 1300 °C, the phase composition of precursor IV.1 tends to equilibrium. The partial transformation of cubic solid solution to monoclinic and tetragonal phase is observed for all compositions. The admixture of low-symmetric phases is estimated as 10-30% depending on the composition. The competitive phase formation in precursor containing 5 mol.% CaO obtained by reverse co-precipitation and further cryochemical dehydration at 400-1300 °C is observed in our recent work [24]. It is interesting to note that final phase composition of precursors II-IV annealed up to 1300 °C is governed in a greater extent by chosen dehydration technique and in a lower extent by the dopant content. Let us mention that the observed phase composition shift in the studied system, i.e. phase formation regularities, and the sequence of phases is determined not only by Gibbs energy change being the thermodynamic factor affecting the process, but also by a number of kinetic parameters: annealing temperature/duration and mean crystallite and aggomerates size in powders. The dispersity of powders (mean agglomerate size) is one of the most important parameters determining the contact area in the reacting powders. As was shown in [26] for quantum dots, the preservation of crystallite size below 14 nm allows kinetic stabilization of intermediate phase formed according to Ostwald step rule. Since nanosized powders are characterized by the excessive energy comparable with the energy of first order transition, phase stabilization of cubic solid solution up to 1000 °C observed by XRD for all precursors can be explained from the positions of mean crystallite and agglomerate size of the powders.

In order to estimate the impact of these kinetic factors, particle size distributions were investigated

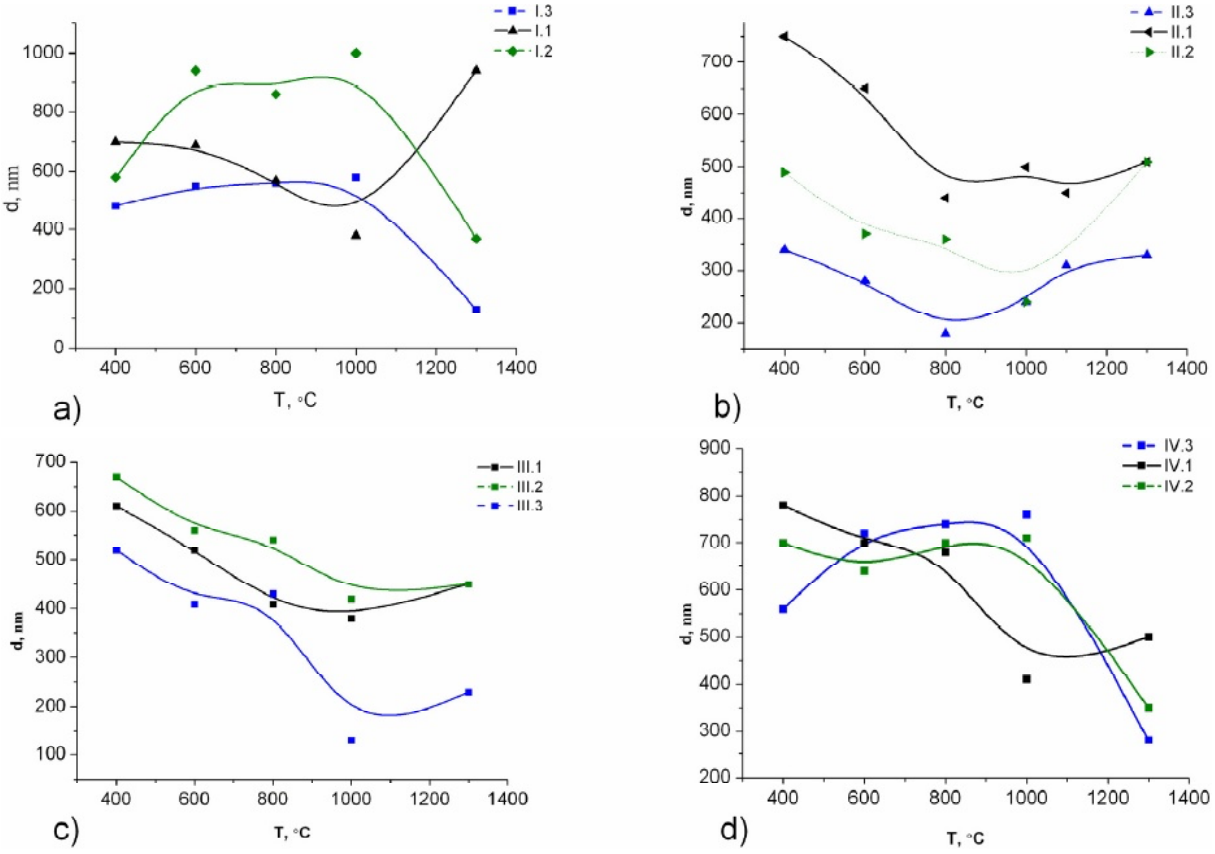

Fig. 4. The dependence of the mean agglomerate size on the annealing temperature for precursors (a) I, (b) II, (c) III, (d) IV.

by PSD analysis, the dependence of mean agglomerate size on annealing temperature is shown in Fig. 4. The data obtained were compared with temperature dependences of mean crystallites size estimated by Scherrer's equation [24,25]. As seen from the figure, the cryochemical dehydration results in fine powders for all compositions studied. Let us note the type of the dependence is similar for all cryochemical techniques used. In general, the regions of deagglomeration and agglomerates baking can be distinguished as it usually takes place in case of pan drying dehydration [21,26]. However, the region corresponding to the deagglomeration here is prolonged until 1000 °C due to crystallization and slow dewatering, while the region corresponding to the baking has a much lower slope. Since the dehydration takes place directly from the solid to gas during freeze-drying, the contact between the particles is eliminated and the particles of dispersed phase in the agglomerate are not bonded by oxygen bridges. The agglomerates break down is due to dehydration and low temperature crystallization taking place already at 360 °C. The formation of cubic solid solution and crystallization takes place up to 800 °C. According to [25], these processes are accompanied by slow crystallite growth and crystallinity increase. The mean crystallite size does not exceed 10-14 nm at 1000 °C. Further temperature increase up to 1300 °C results in slight backing of agglomerates in precursors II and III up to 300-500 nm accompanied by the crystallite growth up to 18-22 nm. It is interesting to note that the mean agglomerate size of stabilized zirconia powders obtained by pan drying and annealing at 1300 °C [23,26] is about 3-4 μm, this is in an order of magnitude higher than the results obtained in the present work. The sharp deagglomeration observed for precursors I and IV in the range 1000-1300 °C cam be assumed as being due to the partial transformation of the metastable cubic solid solution to monoclinic ZrO_2 and the tendency of the composition to the equilibrium. Glycerol addition to the gel prior its freeze-drying (see curves I.3, II.3 and III.3, Fig. 4) favors the agglomerate size decrease for all annealing temperatures. Cryoprotectant addition to the initial gel leads to the changes in freezing, i.e. glycerol addition results in local amorphous regions in the ice. Therefore, the growth of large hexagonal water crystals becomes limited during such freezing. Glycerol molecules prevent

the rejection of the dispersed phase particles from the ice crystals formed. So the freezing takes place homogeneously and is accompanied by smaller ice crystals formation. Summarizing the data of STA, XRD, and PSD-analysis, the following conclusions on the thermodynamic and kinetic factors predetermining the temperature of "amorphous phase → crystalline solid solution" transition in the temperature range from 400 to 1300 °C:

- the difference in the temperature of "amorphous phase → crystalline solid solution" transition does not exceed 20 °C for all compositions after cryochemical dehydration. The value of crystallization enthalpy for this the phase transition can serve as the criterion for crystallization completeness of metastable cubic solid solutions in CaO-ZrO_2 system;
- crystallization and phase formation in the system follows Ostwald step rule and is accompanied by metastable cubic zirconia based solid solution formation. Due to different dehydration degree of powders, freeze-dried powders and powders freeze-dried with glycerol crystallization has a step character, whereas the crystallization is a single step process in case of freezing in liquid nitrogen and pan drying;
- phase stabilization of cubic solid solution is observed in the range 800-1000 °C for compositions I-IV and all dehydration techniques studied, this is due to the fine powders dispersity and small crystallite size (the mean crystallite size being below 14 nm). The onset of cubic solid solution destruction is observed for Specimen I, this process is accompanied by the crystallite mean size increase, the additions of monoclinic ZrO_2 is observed here.
- baking of the agglomerates at 1000-1300 °C is accompanied by slow crystalline growth and partial transformation of cubic solid solution into monoclinic zirconia and equilibrium phase composition formation. Therefore, the formation of metastable phases and step character of crystallization can be regarded as a result of the significant amount of residual water in precursors structure after dehydration. In case of zirconia based precursors, the kinetic factors are critical for metastable crystalline solid solution phase stabilization in a wide range of temperatures and concentrations.

4. CONCLUSIONS

Thermal analysis performed showed that the difference in the temperature of phase transition "amorphous phase → crystalline solid solution" does not exceed 20 °C for each composition after cryochemical dehydration. The value of crystallization enthalpy for this phase transition can serve the criterion for crystallization completeness of metastable cubic solid solutions in CaO-ZrO_2 system. Phase stabilization of the metastable crystalline solid solution at 400-1000 °C and CaO content within 5-15 mol.% is due to kinetic factors such as fine powders dispersity and small crystallite size.

ACKNOWLEDGEMENTS

This research work was supported by the special President's scholarship for young scientists (research project CP-1967.2016.1).

REFERENCES

[1] R. Stevens, *An introduction to zirconia: Zirconia and zirconia ceramics* (Magnesium elektrum, Twickenham, 1986).
[2] S. Akbar, P. Dutta and S. Lee // *Int J Appl Ceram Tech* **3** (2006) 302.
[3] J.W. Fergus // *Sensors and Actuators B: Chem* **121** (2007) 652.
[4] H.J. Neef // *Energy* **34** (2009) 327.
[5] V.G. Konakov, O.Yu. Kurapova, E.N. Solovieva N.N. Novik, M.M. Pivovarov and I.Yu. Archakov // *Materials physics and mecanics* **24** (2015) 340.
[6] I.A. Ovid'ko, A.G. Sheinerman // *Rev. Adv. Mat. Sci.* **39** (2014) 81.
[7] I.A. Ovid'ko // Philosophical Transactions of the Royal Society A: Mathematical, Physical and Engineering Sciences 373 (2015) article number 20140129.
[8] V.G. Konakov, O.Yu. Kurapova, A.R. Arutyunyan, I.V. Lomakin, E.N. Solovyeva, N.N. Novik, I.A. Ovid'ko // *Materials Physicsand Mechanics* **27** (2016) 90.
[9] V.G. Konakov, O.Yu. Kurapova, E.N. Solovyeva, N.N. Novik, M. M. Pivovarov, I.A. Ovid'ko // *Materials Physics and Mechanics* **24** (2015) 331.
[10] V.G. Konakov, I.A. Ovid'ko, O.Yu. Kurapova, N.N. Novik, I.Yu. Archakov // *Materials Physics and Mechanics* **21** (2014) 305.
[11] V.G. Konakov, O.Yu. Kurapova, I.V. Lomakin, E.N. Solovieva, I.Yu. Archakov, I.A. Ovid'ko // Rev Adv Mat Sci 44 (2016) 361.
[12] N.N. Novik, V.G. Konakov and I.Yu. Archakov // *Rev Adv Mater Sci* **40** (2015) 188.

[13] O.Yu. Kurapova and V.G. Konakov // *Rev. Adv. Mater. Sci.* **36** (2014) 176.
[14] D. Gazzoli, G. Mattei and M. Valigi // *J Raman Spectrosc* **38** (2007) 824.
[15] N.M. Sammes, G.A. Tompsett, H. Nafe and F. Aldinger // *J Eur Ceram Soc* **19** (1999) 1801.
[16] A.C. Geiculescu and H. Rack // *J Sol-gel Sci Technol* **20** (2001) 13.
[17] H.J. Schmidt // *J Sol-gel Sci Technol* **40** (2006) 115.
[18] P. Buhler, *Nanothermodynamics* (Yanus, St. Petersburg, 2004).
[19] D.J. Kim, H.J. Jung and I.S. Yang // *Journal of the American Ceramic Society* **76** (1993) 2106.
[20] W. Pyda, K. Haberko and M.M. Bułko // *J Amer Ceram Soc* **74** (1991) 2622.
[21] V.S. Stubican and S.P. Ray // *J. Am. Ceram. Soc.* **60** (1977) 535.
[22] O. Yu. Kurapova, V. G. Konakov, S. N. Golubev, E.N. Solovieva and V. M. Ushakov // *Bull. St. Petersburg University* **4** (2013) 72.
[23] R. Morrison and R. Boid*, Organic chemistry* (Mir, Moscow, 1974), In Russian. [18] O.Yu. Kurapova, V.G. Konakov, S.N. Golubev and V.M. Ushakov // *Refractories and Industrial Ceramics* **55** (2014) 151.
[24] O.Yu. Kurapova, V.G. Konakov, S.N. Golubev and V.M. Ushakov // *Bull. St. Petersburg University **4*** (2016) 296.
[25] O.Yu. Kurapova, V.G. Konakov, D.V. Nechaeva, A. V. Ivanov and S.N. Golubev, V.M. Ushakov // *Rev. Adv. Mater. Sci.* **47** (2016).
[26] V.G. Konakov, S. Seal, E.N. Solovieva, S.N. Golubev, M.M. Pivovarov and A.V. Shorochov // *Rev. Adv. Mater. Sci.* **13** (2006) 71.
[27] A.L. Washington, M.E. Foley, S. Cheong, L. Quffa, C.J. Breshike, J. Watt ... and G. Strouse // *Journal of the American Chemical Society* **134** (2012) 17046.